Experimental foundation and constitutive equations of multisurface theory of plasticity with one active surface

Boris E. Melnikov Igor N. Izotov Artem S. Semenov Sergey G. Semenov
Sergey V. Petinov
kafedra@ksm.spbstu.ru

Abstract

The multisurface theory of plasticity with one active surface of equal plastic compliances is aimed to describe the elastic-plastic deformation under complex passive loading paths. Tensor and vector forms of constitutive equations are proposed. The conditions of thermodynamical consistency of the theory are obtained. A generalization of the theory for the case of arbitrary shape of surfaces with equal compliances and of the anisotropy of elastic properties were carried out. Surfaces of equal compliances for the multilink loading paths and for the complex cyclic loading with total and partial unloading are experimentally studied. Comparison of experimental data and theory predictions was carried out.

Introduction

The theory of plastic flow with the isotropic-kinematic hardening is not sufficiently reliable [1] for the description of deformation processes under the loading including partial or complete unloading after sharp breaks of loading path. Typically, the models of plasticity are aimed for the improved description of the active loading. The detailed analysis of the passive loading is attempted only occasionally, and mostly is limited by an assumption of elastic behavior of material at the unloading.

The multisurface theory of plasticity with one active surface [2, 3, 4] provides more precise formulation of the passive loading. Another specific feature of the theory version is the refusal of application of the yield surface for evaluation of plastic deformation. The disadvantage of the yield surface is that its shape, size and location depend on the off-set of the residual strain. This disadvantage is avoided when the surfaces of equal plastic compliances are applied as it is done in the considered theory. The principle of building of the surfaces of equal plastic compliances is shown in Fig. 1.

The principal for theory reversing conditions and constitutive equations were derived based on analysis of experimental data.

The multisurface theory with one active surface plays a key role in the multimodel analysis [5] of plastic deformation, which is based on the use of a hierarchical sequence of models adequate to complexity of the problem.

1 Conditions of reversing

Reversing is one of the basic concepts in the theory. The loading paths are assumed piecewise smooth in the space of the stress tensor deviators. The subset of loading path

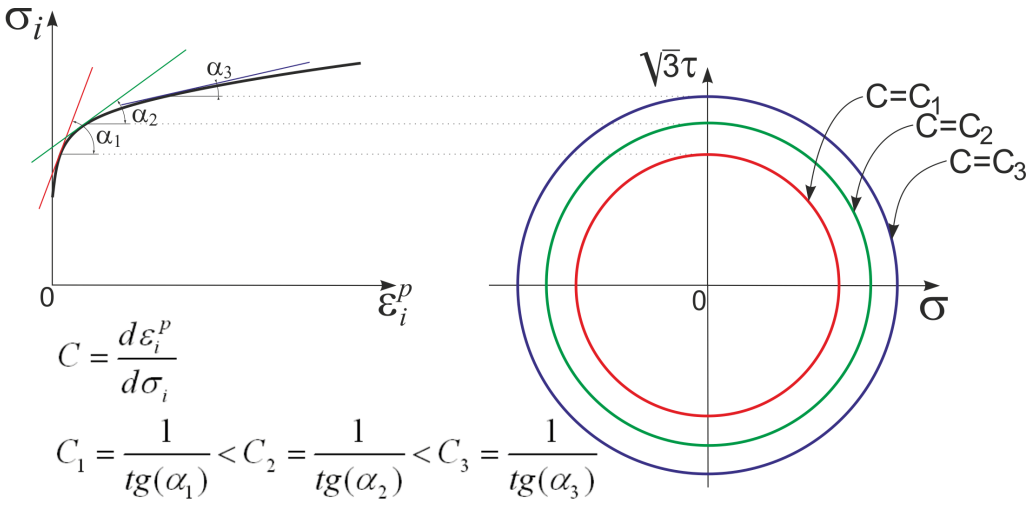

Figure 1: Surfaces of equal plastic compliances.

kinks, after which the following stress development is directed inside the surface of equal compliance, is defined as a reversing points of the loading path ($\boldsymbol{\sigma}_{R_1}$ and $\boldsymbol{\sigma}_{R_2}$ in Fig. 2).

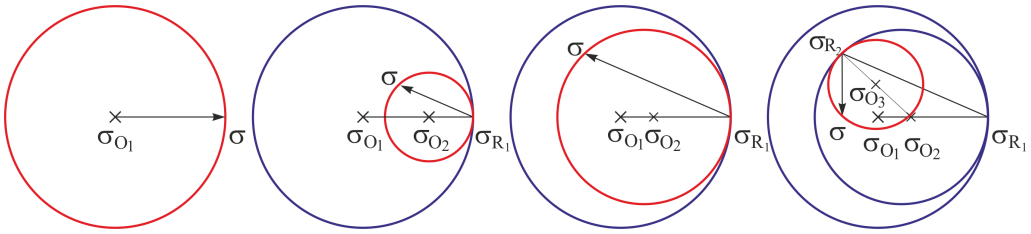

Figure 2: Illustration of the reversing points birth and the evolution of corresponding surfaces of equal plastic compliances.

Condition for initiation of a k-th new reversing is defined as follows:

$$\frac{\partial f_k(\boldsymbol{\sigma} - \boldsymbol{\sigma}_{Ok})}{\partial \boldsymbol{\sigma}} \cdot\cdot\, d\boldsymbol{\sigma} < 0, \tag{1}$$

where $\boldsymbol{\sigma}$ is the stress tensor, $\boldsymbol{\sigma}_{Ok}$ is the center of a k-th surface of equal plastic compliances which characterizes its translation as of a rigid body. An occurrence of a new k-th reversing point, $\boldsymbol{\sigma}_{R_k}$, causes developments of a new k+1-st surface:

$$F_{k+1}(\boldsymbol{\sigma}_A, \boldsymbol{\sigma}_{R_j}, \boldsymbol{\varepsilon}^p) = f_{k+1}(\boldsymbol{\sigma}_A) - \psi_{k+1}(\boldsymbol{\sigma}_{R_j}, \boldsymbol{\varepsilon}^p) = 0, \qquad j = \overline{1,k} \tag{2}$$

which determines the plastic deformation. The tensor of active stress is defined by the relation $\boldsymbol{\sigma}_A = \boldsymbol{\sigma} - \boldsymbol{\sigma}_{O_{k+1}}$. In equation (2) $\boldsymbol{\sigma}_{R_j}$ is the stress at j-th reversing point, $\boldsymbol{\varepsilon}^p$ is the plastic strain tensor.

The birth condition of the first reversing point according to (1) at k=1 coincides with condition for elastic unloading, postulated in the flow theory; however, in the multisurface theory the reversing is accompanied by continuation of plastic deformation.

A family of k+1 surfaces occurs after appearance of k reversing points on the loading path. Initial surface, F_1, has a non-reversing initiation and its evolution is defined by the stress-strain curve, as in the flow theory as well. An active surface, i.e. changing its dimensions and controlling plastic deformation is the ultimate surface, F_{k+1}; parameters of all preceding surfaces remain unchanged. These surfaces are nested: every preceding

surface completely envelops successive one. So far, the active surface initially has minimal dimensions, but in loading it grows up and may become equal to the preceding surface. This issue is classified as a deletion of the conclusive k-th reversing point; the F_k-surface becomes an active surface instead of the F_{k+1}-surface. The deletion is defined by coinciding of k+1-th and k-th surfaces:

$$f_{k+1}(\boldsymbol{\sigma} - \boldsymbol{\sigma}_{O_{k+1}}) = f_k(\boldsymbol{\sigma}_{R_k} - \boldsymbol{\sigma}_{O_k}). \tag{3}$$

This relationship is applicable when evolution of surfaces is limited by similitude and translation transformations.

2 Constitutive equations

Constitutive equations taking into account the elastic anisotropy and arbitrary shape of the surfaces are given as [4]:

$$d\boldsymbol{\sigma} = \boldsymbol{D} \cdot\cdot (d\boldsymbol{\varepsilon} - d\boldsymbol{\varepsilon}^p), \tag{4}$$

$$d\boldsymbol{\varepsilon}^p = C \frac{\partial f(\boldsymbol{\sigma}_A)}{\partial \boldsymbol{\sigma}} \frac{\partial f(\boldsymbol{\sigma}_A)}{\partial \boldsymbol{\sigma}} \cdot\cdot d\boldsymbol{\sigma}, \tag{5}$$

where $\boldsymbol{\varepsilon}$ and $\boldsymbol{\varepsilon}^p$ are the total and plastic strain tensors, the condition $f(\boldsymbol{\sigma}_A) = f_{k+1}(\boldsymbol{\sigma}_A)$ corresponds to k+1-th active surface, C is the modulus of plastic compliance, $\boldsymbol{D}$ is the tensor of elastic moduli, in case of isotropic material defined by the Young's modulus and Poisson's ratio.

When the surface of equal compliance is assumed as von-Mises hypersphere,

$$f(\boldsymbol{\sigma}_A) = f(\boldsymbol{s}_A) = \sqrt{3/2 \boldsymbol{s}_A \cdot\cdot \boldsymbol{s}_A}, \tag{6}$$

where $\boldsymbol{s}_A$ is the deviator of the active stress tensor $\boldsymbol{\sigma}_A$, then the flow condition (5) would become:

$$d\boldsymbol{\varepsilon}^p = 3/2 C \frac{\boldsymbol{s}_A \boldsymbol{s}_A \cdot\cdot d\boldsymbol{s}}{\boldsymbol{s}_A \cdot\cdot \boldsymbol{s}_A}. \tag{7}$$

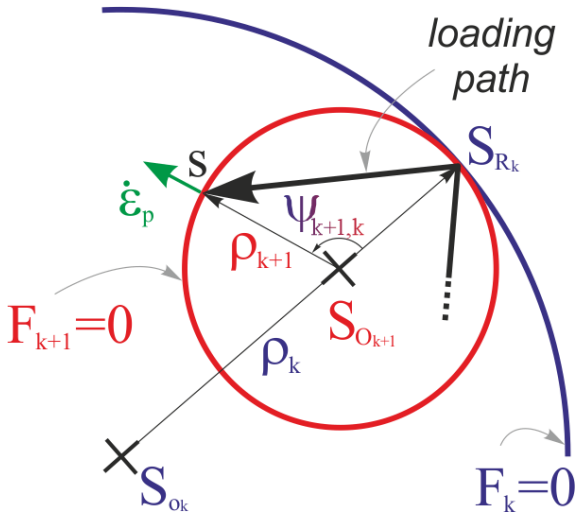

Figure 3: Surfaces of equal plastic compliances.

If the hypothesis (7) is applied then the process of plastic deformation is completely defined in the five-dimensional space of stress deviators (Fig. 3). Therefore the equations of evolution of equal compliance surfaces and reversing conditions are defined in this case by deviatoric components of tensors $\boldsymbol{\sigma}, \boldsymbol{\sigma}_A, \boldsymbol{\sigma}_{R_j}, \boldsymbol{\sigma}_{O_j}$, denoted, respectively, as $\boldsymbol{s}, \boldsymbol{s}_A, \boldsymbol{s}_{R_j}, \boldsymbol{s}_{O_j}$. Centers of von-Mises hyperspheres is defined by equations:

$$\boldsymbol{s}_{O_{j+1}} = \boldsymbol{s}_{O_j} + a_j(\boldsymbol{s}_{R_j} - \boldsymbol{s}_{O_j}), \quad a_j = \frac{(\boldsymbol{s}_{R_{j+1}} + \boldsymbol{s}_{R_j} - 2\boldsymbol{s}_{O_j}) \cdot\cdot (\boldsymbol{s}_{R_{j+1}} - \boldsymbol{s}_{R_j})}{2(\boldsymbol{s}_{R_j} - \boldsymbol{s}_{O_j}) \cdot\cdot (\boldsymbol{s}_{R_{j+1}} - \boldsymbol{s}_{R_j})}. \tag{8}$$

The surface equation (2) is simplified to:

$$F_{k+1} = \sqrt{3/2\boldsymbol{s}_{A_{k+1}} \cdot\cdot \boldsymbol{s}_{A_{k+1}}} - Y_{k+1} = 0, \quad Y_{k+1} = \sqrt{3/2}\rho_{k+1}. \tag{9}$$

The radius of j-th passive surface is given by:

$$\rho_j = \sqrt{\boldsymbol{s}_{P_j} \cdot\cdot \boldsymbol{s}_{P_j}} = \sqrt{(\boldsymbol{s}_{R_j} - \boldsymbol{s}_{O_j}) \cdot\cdot (\boldsymbol{s}_{R_j} - \boldsymbol{s}_{O_j})}. \tag{10}$$

The radius of k+1-th active surface is defined by similar expression:

$$\rho_{k+1} = \sqrt{\boldsymbol{s}_{A_{k+1}} \cdot\cdot \boldsymbol{s}_{A_{k+1}}} = \sqrt{(\boldsymbol{s} - \boldsymbol{s}_{O_{k+1}}) \cdot\cdot (\boldsymbol{s} - \boldsymbol{s}_{O_{k+1}})}. \tag{11}$$

The nesting condition requires the fulfillment of inequalities: $0 < \rho_{k+1} < \rho_k < ... < \rho_2 < \rho_1$.

It was shown [5], that the multisurface theory with one active surface satisfies to the thermodynamic constraints in a form of the dissipative inequality:

$$\boldsymbol{\sigma} \cdot\cdot \dot{\boldsymbol{\varepsilon}} - \rho\dot{\psi} \geq 0 \tag{12}$$

if the plastic compliance is approximated as

$$C_{k+1} = \begin{cases} C_1(\frac{\rho_{k+1}}{\rho_1})^N & \text{if } \rho^{**}_{k+1} \leq \rho_k \\ C_1 \frac{\rho_k - \rho_{k+1}}{\rho_1}(\frac{\rho_{k+1}}{\rho_1})^N & \text{if } \rho^{**}_{k+1} > \rho_k \end{cases}, \tag{13}$$

where $\rho^{**}_{k+1} = -\frac{1}{1-cos\psi_{k+1,k}}[\rho_k cos\psi_{k+1,k} + \sum_{j=1}^{k-1}(\rho_j - \rho_{j+1})cos\psi_{k+1,j}]$, ρ is the material density, ψ is the specific free energy.

3 Experimental analysis

The program of experimental studies includes complex loading tests of thin wall tubular steel specimens (tension, internal and external pressure) and tubular pure nickel specimens (tension and torsion).

3.1 Test results for specimens made of pure nickel

Specimen particulars: thin wall tubular, outer diameter 8.1 mm, wall thickness 0.19 mm (not less than 6-7 grains), gage length 150 mm, material is are pure nickel (impurities: Si - 0,068%; Fe - 0,025%; Cu - 0,02%). A tolerance on the tube cylindricity does not prevail ±0,01 mm (±0,1%); maximum deviation of crossection area in the same specimen was achieved about ±0,03 mm^2 (±0,7%). Specimens were annealed at 860°C and cooled in furnace.

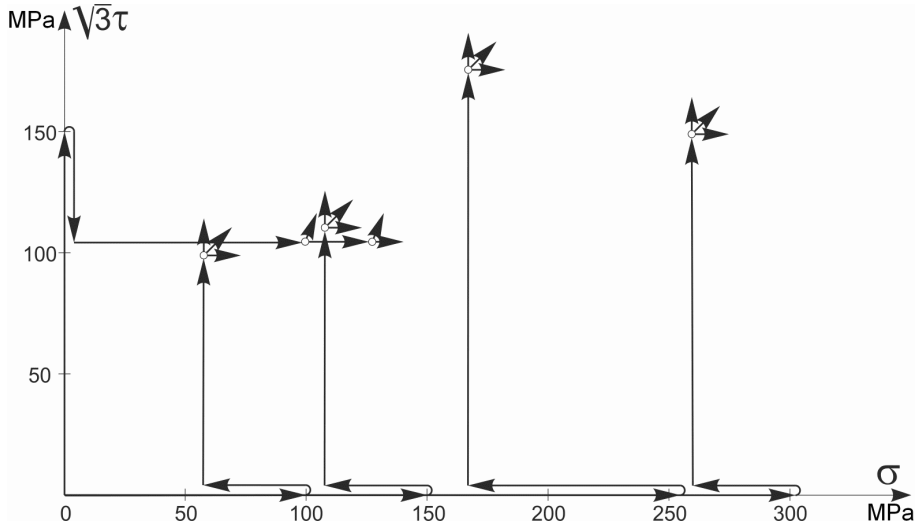

Figure 4: Loading paths for nickel specimens.

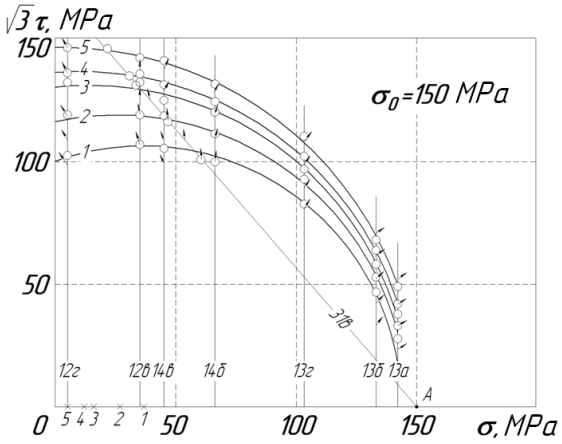

Figure 5: Axial loading.

$$C_1 = 1 \cdot 10^{-11}\, Pa^{-1}$$
$$C_2 = 2 \cdot 10^{-11}\, Pa^{-1}$$
$$C_3 = 3 \cdot 10^{-11}\, Pa^{-1}$$
$$C_4 = 5 \cdot 10^{-11}\, Pa^{-1}$$
$$C_5 = 10 \cdot 10^{-11}\, Pa^{-1}$$

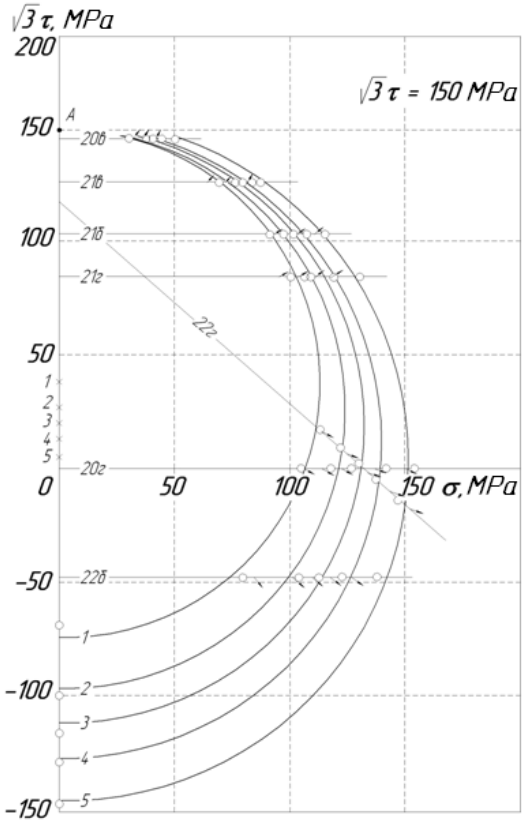

Figure 6: Torsion.

Tests were carried out for five versions of loading with initial von Mises stresses corresponding to: 105 MPa, 150 MPa (tension and torsion), 258 MPa and 306 MPa, which were attained in different paths as shown in Fig. 4.

Comparison of various models predicitions with experimental data for for the nickel specimen under complex loading path is presented in Fig. 7.

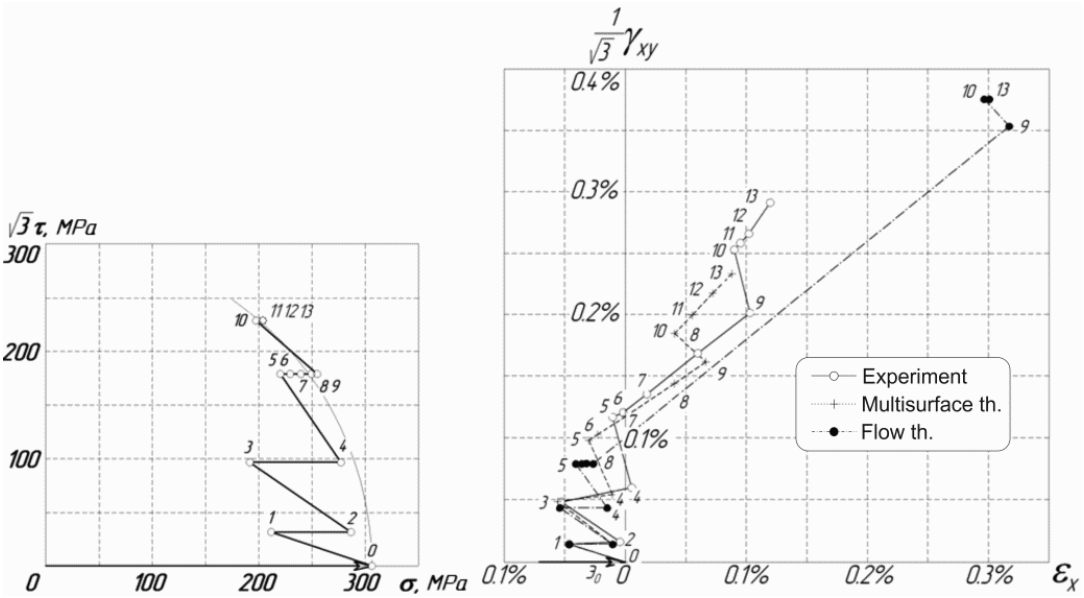

Figure 7: Comparison of computed and experimental data for nickel specimen.

3.2 Test results for specimens made of steel X18H10T

A check of the unified curve hypothesis consistency, a stability of the stress-strain curve, a robustness of approximation of the modulus C, an evaluation of hydrostatic pressure influence were carried out.

Experimental data and results of calculations with different theories are compared in Fig. 9 for the loading path shown in Fig. 8. Results of the comparison indicate a good accuracy of the multisurface theory with one active surface.

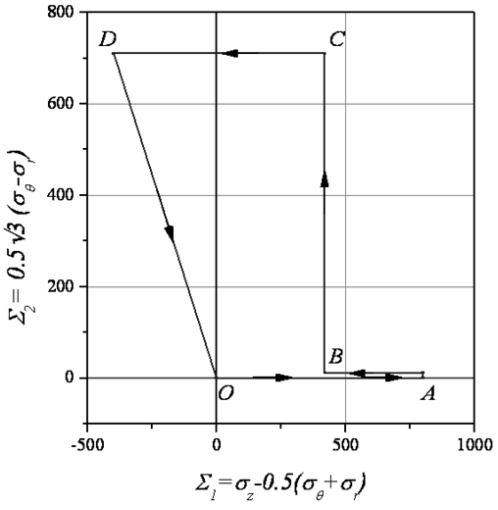

Figure 8: Loading path for steel specimen.

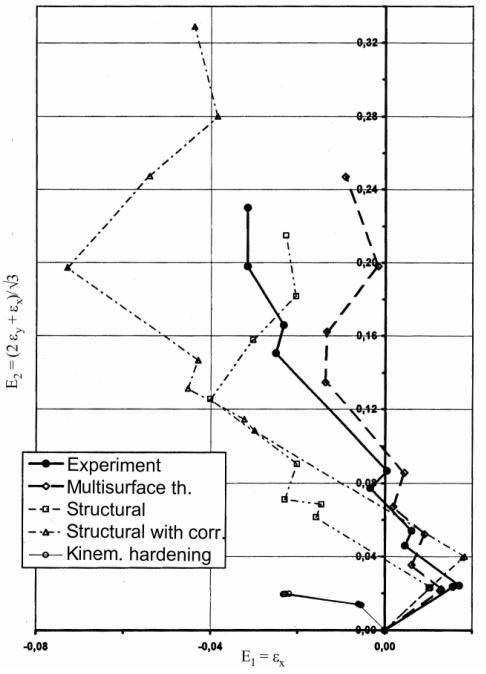

Figure 9: Comparison of computed and experimental data for steel specimen.

4 Numerical implementation of the constitutive equations

In the presence of k reversing points on the loading path 2k+3 situations are possible at the current loading step:

- No a birth and deletion of reversing points;
- A birth of a new k+1-th reversing point;
- k cases of simultaneous deletions from one to k reversing points;
- k+1 cases of a birth of k+1-th reversing point after preceding deletion from one to k+1 reversing points.

The loading step is subdivided into sub-steps with aim to take into account mentioned peculiarities. The points of intersection of the stress path with deletable surfaces are defined by the equation $\boldsymbol{s}^i_{l+1} = \boldsymbol{s}_l + \alpha^i(\boldsymbol{s}_{l+1} - \boldsymbol{s}_l)$ with:

$$\alpha^i = -\frac{\left(\boldsymbol{s}_l - \boldsymbol{s}_{O_{k+1-i}}\right)\cdot\cdot\Delta\boldsymbol{s}}{\Delta\boldsymbol{s}\cdot\cdot\Delta\boldsymbol{s}} + \sqrt{\left[\frac{\left(\boldsymbol{s}_l - \boldsymbol{s}_{O_{k+1-i}}\right)\cdot\cdot\Delta\boldsymbol{s}}{\Delta\boldsymbol{s}\cdot\cdot\Delta\boldsymbol{s}}\right]^2 + \frac{\rho^2_{R_{k+1-i}} - \rho^2_l}{\Delta\boldsymbol{s}\cdot\cdot\Delta\boldsymbol{s}}} \tag{14}$$

where $\rho_{R_{k+1-i}} = \sqrt{\left(\boldsymbol{s}_{R_{k+1-i}} - \boldsymbol{s}_{O_{k+1-i}}\right)\cdot\cdot\left(\boldsymbol{s}_{R_{k+1-i}} - \boldsymbol{s}_{O_{k+1-i}}\right)}$,

$\rho_l = \sqrt{\left(\boldsymbol{s}_l - \boldsymbol{s}_{O_{k+1-i}}\right)\cdot\cdot(\boldsymbol{s}_l - \boldsymbol{s}_{O_{k+1-i}})}$.

5 The finite-element implementation

The constitutive equations (4) - (7) represent quasilinear differetial-algebraic equations and admit to obtain exactly tangent moduli and algorithmically consistent tangent moduli, which allows to use of effective methods (e.g., Newton-Raphson method) for the solution of nonlinear finite element (FE) equations. The conditions for reversing were analyzed in cases of small and finite load increments. The constitutive equations of multisurface theory have been implemented in the FE programm PANTOCRATOR [7] and solutions of non-linear boundary value problems have been obtained (see Fig. 10).

Conclusion

A thermodynamically consistent theory of plasticity is developed, friendly to application in the finite-element analysis. The theory allows development of plastic deformation at the passive loading that is essential in case of the low-cycle fatigue analysis. The results of computations based on the proposed theory reasonably good fit the results of experimental studies.

Acknowledgements

The study was supported by RFBR, research project 12-08-00-943a.

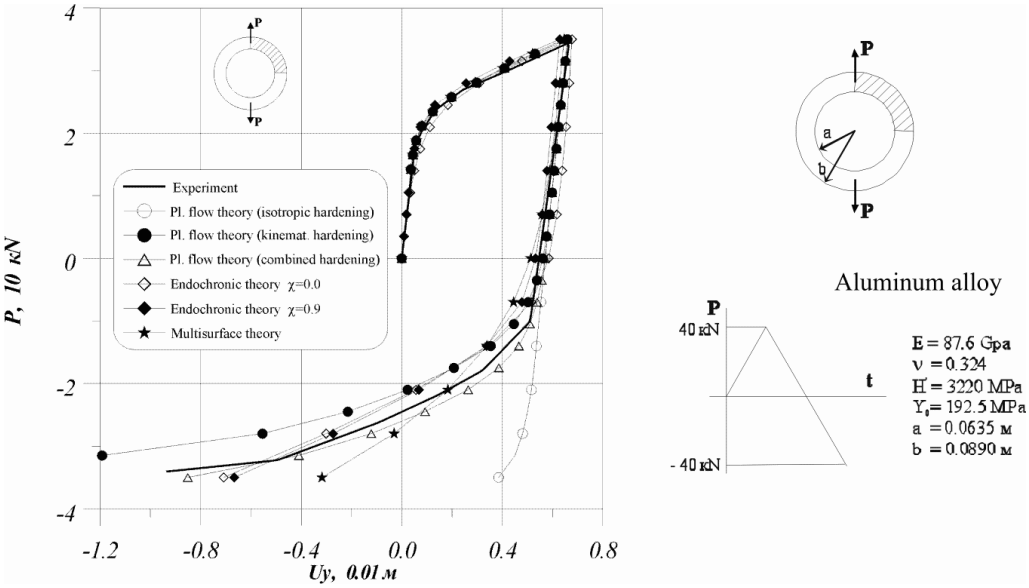

Figure 10: Comparison of the FE analysis results for an aluminium ring under uniaxial tension/compression with experimental data [8].

References

[1] H. S. Lamba and O. M. Sidebottom. Cyclic Plasticity for Nonproportional Paths: Part 2 — Comparison With Predictions of Three Incremental Plasticity Models // J. Eng. Mater. Technol. 1978. 100(1). P. 104-111. doi:10.1115/1.3443440

[2] Izotov I.N., Yagn Ju.I. Analysis of plasticity preceded by imposed anisotropy // Reports of Academy of Sciences of USSR. 1961. Vol. 139. № 3. P. 575-579. (in Russian)

[3] Melnikov B.E., Izotov I.N. and Kuznetsov N.P. Calculation and experimental examination of complex modes of elastoplastic deformation // Strength of Materials. 1990. 22(8). P. 1122-1127. doi:10.1007/BF00767741

[4] Melnikov B.E. and Semenov A.S. Evolution of Equal Compliance Surfaces in the Multisurface Theory of Plasticity // Transactions of St.-Peterburg State Polytechnic University. 1996. Vol. 456. P. 52-61. (in Russian)

[5] Melnikov B.E., Semenov A.S., Semenov S.G. Multimodel analysis of elastic-plastic deformation of materials and structures // Proceedings of the A.N. Krylov Shipbuilding Research Institute. 2010. № 53. pp. 85-92. (in Russian)

[6] Semenov A.S. Thermodynamic Consistency of the Multisurface Theory of Plasticity with One-active Surface // Scientific and technical Bulletin of St.-Peterburg State Polytechnic University. 2003. Vol.33, № 3. P. 103-114. (in Russian)

[7] Semenov A.S. PANTOCRATOR - the finite element programm specialized on the nonlinear problem solution. Proceedings of the Vth international conference on scientific and engineering problems of predicting the reliability and service life of structures. St.-Peterburg. 2003. P. 466-480. (in Russian)

[8] Owen D.R.J., Prakash A., Zienkiewicz O.C. Finite element analysis of non-linear composite materials by use of overlay systems. Computers & Structures, 1974, Vol. 4, P. 1251в Ъ“1267

Experimental foundation and constitutive equations of multisurface theory of plasticity with one active surface

Boris E. Melnikov, Politechnicheskaya str. 29, Saint-Petersburg, Russia
Igor N. Izotov, Politechnicheskaya str. 29, Saint-Petersburg, Russia
Artem S. Semenov, Politechnicheskaya str. 29, Saint-Petersburg, Russia
Sergey G. Semenov, Politechnicheskaya str. 29, Saint-Petersburg, Russia
Sergey V. Petinov, Politechnicheskaya str. 29, Saint-Petersburg, Russia